
1

AN INTRODUCTION TO MOLECULAR IMAGING

GA-LAI LAW AND WING-TAK WONG

Department of Applied Biology and Chemical Technology, Hong Kong Polytechnic University, Hung Hom, Kowloon, Hong Kong SAR, China

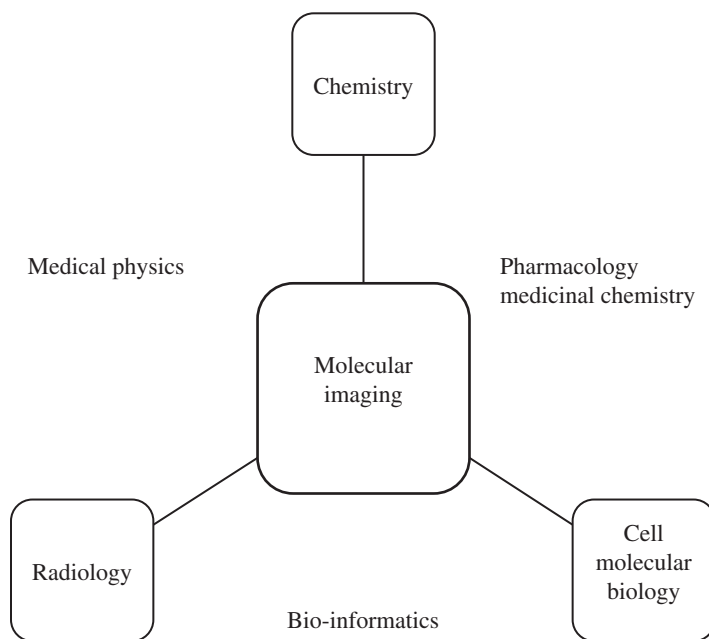
1.1 INTRODUCTION

The aim of this book is to introduce the concepts of different imaging techniques that are employed for diagnostics and therapy and the role that chemistry has played in their evolution. The book provides a general introduction to the area of molecular imaging, giving an account of the role of molecular design and its importance in modern-day techniques, with an in-depth introduction of some of the probes and methodologies employed. This first chapter introduces the different types of imaging modalities currently at the forefront of imaging and illustrates some basic concepts underlying these techniques. It acts as a simplified background to set the scene for the following chapters, which will discuss the chemical properties of molecules and the role they play in different imaging modalities. For the interested readers, other textbooks are referenced that will provide more detailed information regarding the different techniques reviewed.

In life everything is incessantly changing. There is constant evolution in life sciences, evolution in the way problems arise, and evolution in the way they are solved. Diagnostics and therapy are both important, but as Einstein said, “intellectuals solve problems, geniuses prevent them.” The key challenge still remains to unravel the hidden knowledge within life sciences, which constantly challenges us with new diseases and mechanistic mutation of biological systems and pathways [1]. Again, as stated by Einstein, “once we accept our limits, we go beyond them.”

Molecular imaging aims to detect and monitor mechanistic processes in cells, tissues, or living organisms with the use of instruments and contrast mechanisms without perturbing their living system. Ultimately, it is a field that utilises molecular building blocks to bring solutions to problems by specialised imaging techniques that have matured into a large integrated field enveloped within various branches of science (Figure 1.1) [2]. In the area of modern-day imaging where technology is at its pinnacle, molecular design still holds a dominant role in the forefront of molecular imaging.

In the past, developments in contrast agents, probes, and dyes have brought about an era of creativity where new techniques, materials, and designs have flourished to form a concrete foundation resulting in today’s achievements in diagnosis and therapy (Figure 1.2). The construction of better chemical molecules will continue to help us develop a more comprehensive picture of learning about life science. Figure 1.3 depicts a timeline in the development of the field [1–3].



Visual representation of cellular and molecular processes within intact living organisms

FIGURE 1.1 Types of multidisciplinary fields related to molecular imaging.

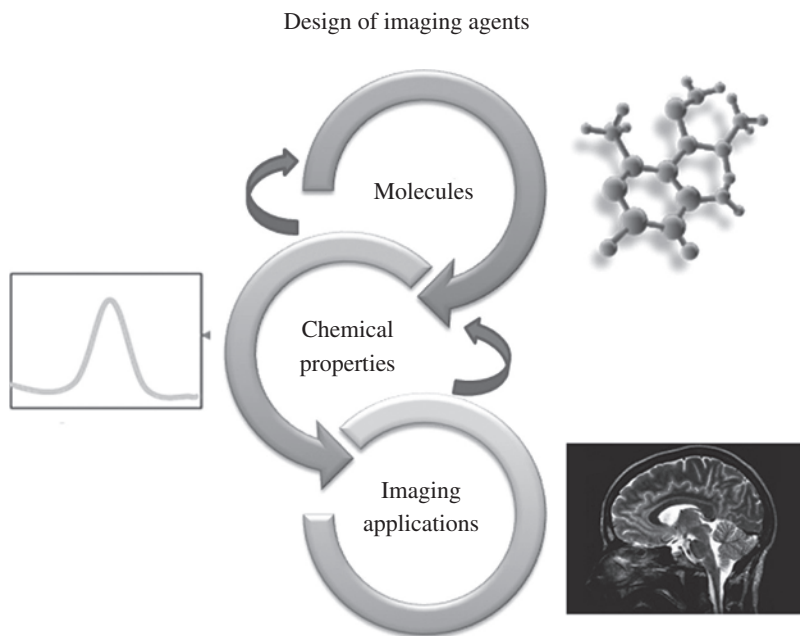


FIGURE 1.2 Diagram showing the links in the design rationale of imaging agents.

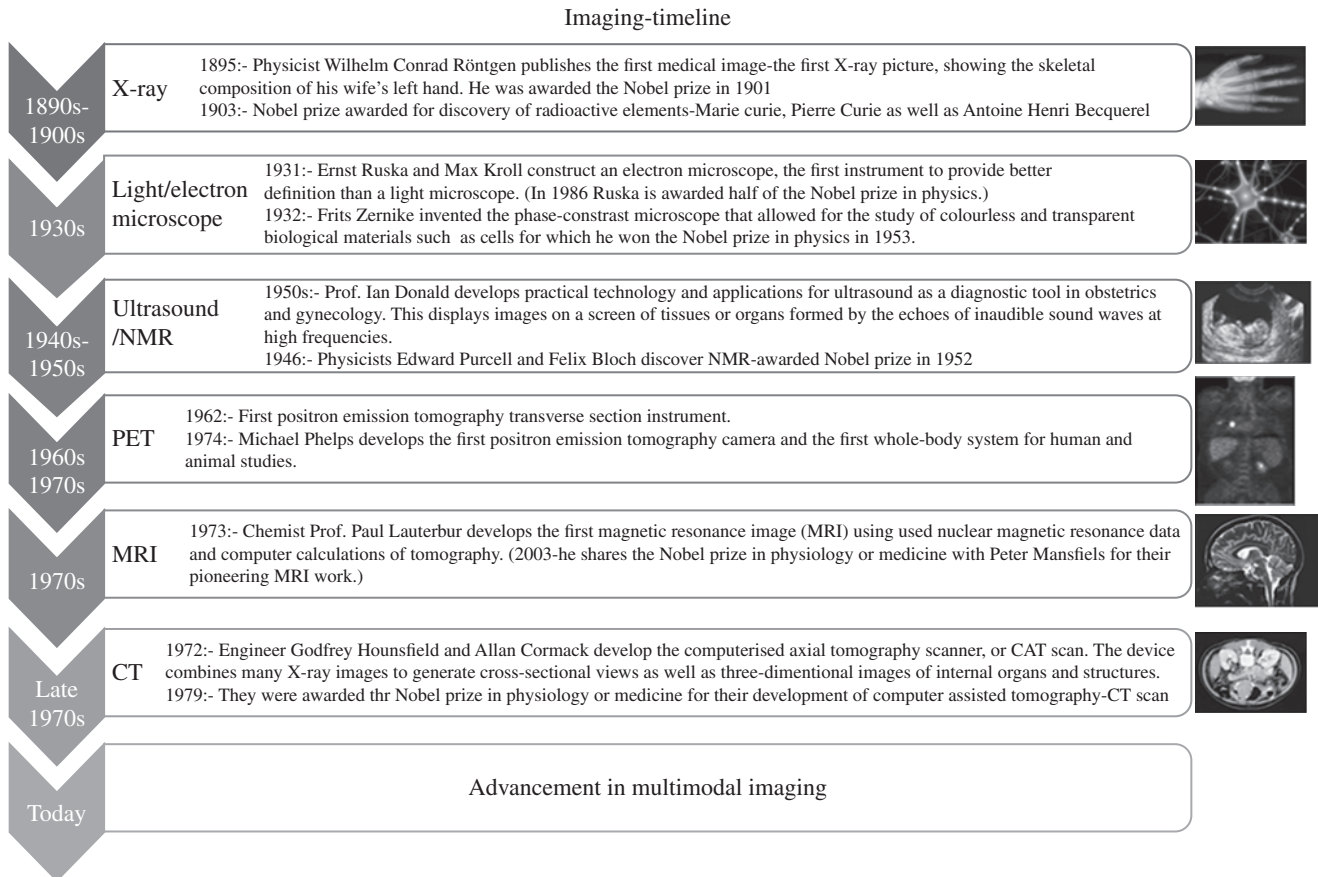


FIGURE 1.3 An approximate timeline showing the development of the different imaging modalities [1–3].

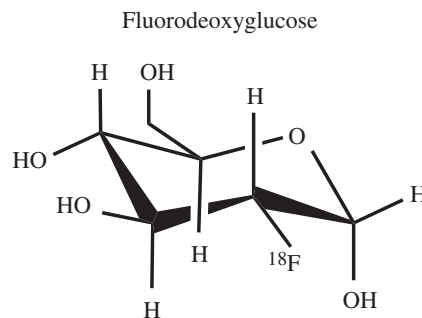


FIGURE 1.4 ^{18}F FDG, a typical contrast agent used in PET.

1.2 WHAT IS POSITRON EMISSION TOMOGRAPHY (PET)?

Positron Emission Tomography (PET) is a nuclear medicine tomographic modality and one of the most sensitive methods for quantitative measurement of physiologic processes *in vivo* [4]. This technique utilises positron-emitting radionuclides and requires the use of radiotracers that decay and produce two 511 keV γ -rays resulting from the annihilation of a positron and an electron. One of the most commonly used molecules is ^{18}F -labelled fluorodeoxyglucose (^{18}F FDG), which has radioactive fluorine and is readily taken up by tumours (Figure 1.4) [5].

1.2.1 Basic Principles

In PET, a neutron-deficient isotope causes positron annihilation to produce two 511 keV γ -rays, which are simultaneously emitted when a positron from a nuclear disintegration annihilates in tissue. PET imaging, unlike MRI, ultrasound, and optical imaging, does not require any external sources for probing or excitation; instead, the source is generated from radioisotopes and emitted from

but not transmitted through an object/patient, as in CT imaging [4–7]. Radionuclides are incorporated as part of a small metabolically active molecule to generate radiotracers such as ^{18}F FDG, which are then intravenously injected into patients at trace dosage for PET imaging. ^{18}F FDG is a favourable radiotracer because it is inhibited from metabolic degradation before it decays due to the fluorine at the 2' position in the molecule. Upon decay, the fluorine is converted into ^{18}O . There is generally a short period of time before accumulation of radiotracers into the targeted organs or tissues that are being examined, so it is important for radiotracers to have a suitable half-life—some commonly used radionuclides have very short half-lives. Some common radionuclides used in PET are ^{11}C (half-life ~20 min), ^{13}N (~10 min), ^{15}O (~2 min) and ^{18}F (~110 min). These are produced by a cyclotron, whereas ^{82}Rb (76 s), which is used in clinical cardiac PET, is produced by a generator [8–9].

When a radioisotope undergoes positron emission decay (positive β -decay), it emits a positron that travels through the tissue for a short distance ($\sim < 2$ mm) whilst decelerating by the loss of its kinetic energy until it collides with an electron. This results in back-to-back annihilation of γ -ray photons, which move in opposite directions and are emitted nearly 180 degrees apart before being detected by scintillators and a photomultiplier tube. This type of coincidence is a true coincidence event; to detect this, the detectors are designed like a ring that surrounds the patient during the scanning procedure. Several parallel rings form the complete detection panel of the PET system in a cylindrical geometry (Figure 1.5).

PET has relatively high sensitivity in detecting molecular species (10^{-11} – 10^{-12} M), even though not all annihilation photons are used for image reconstruction because not all coincidences are true coincidences. A coincidence event is assigned to a line of response where the two relevant detectors are joined (detectors opposite to each other); this allows for positional information to be located from the detected radiation without any physical collimators. This is known as electronic collimation. There are four types of coincidence events in PET: true, scattered, random, and multiple (Figure 1.6). Only true coincidence, which is the simultaneous detection of two emissions from a single annihilation event, is useful. No other events are detected within this coincidence time-window.

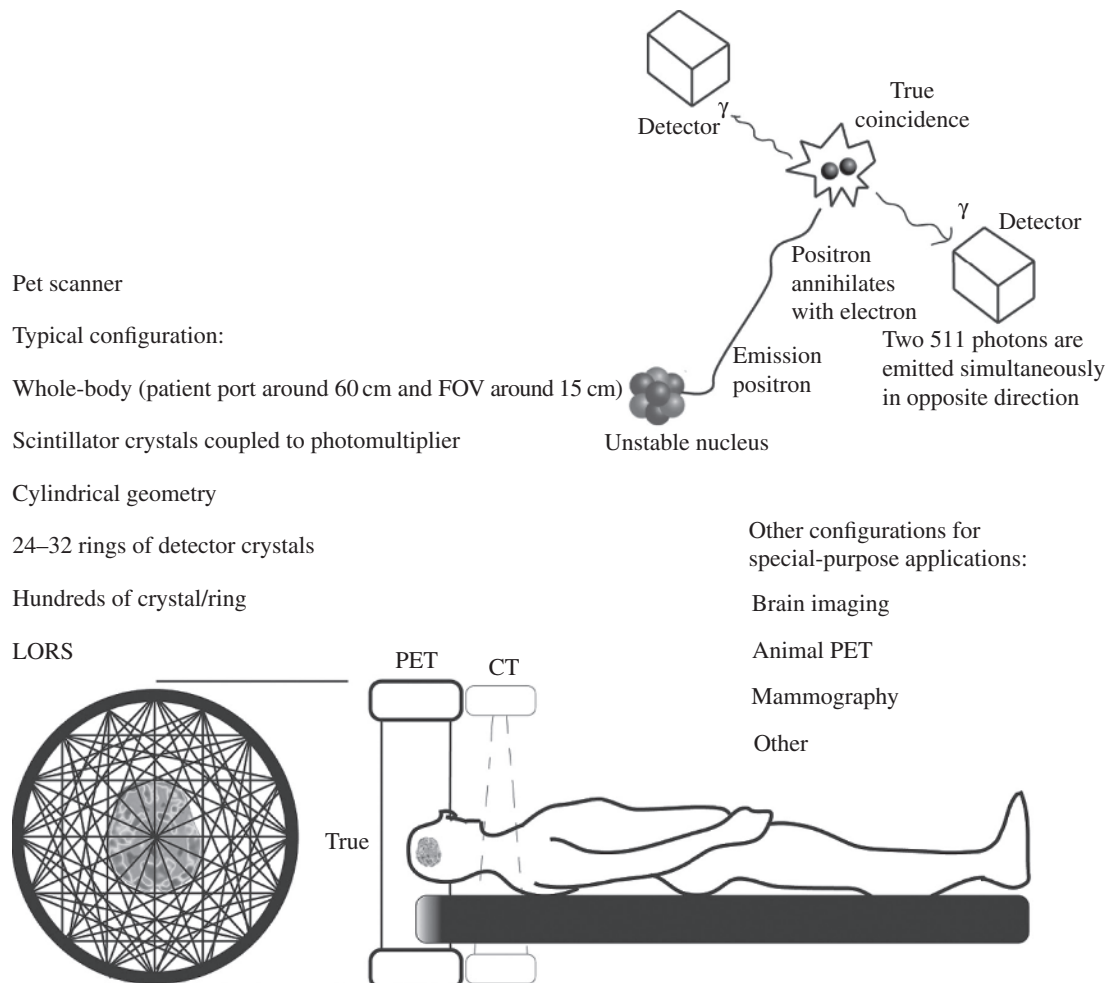


FIGURE 1.5 Typical configuration of a PET scanner.

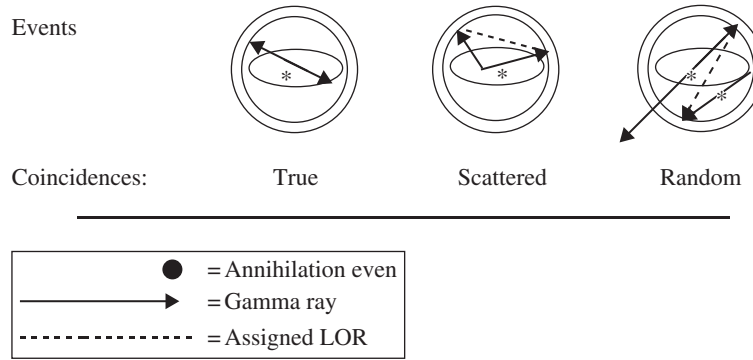


FIGURE 1.6 Different types of coincidence events.

Scattered coincidence occurs when one or both photons from a single event are scattered and both are detected; however, one of the photons must have undergone at least one Compton scattering event prior to detection. This type of event adds a background to the true coincidence event and causes overestimation of the isotope concentration as well as decreasing image contrast. In Compton scattering, a photon interacts with an electron in the absorber material, resulting in an increase in the kinetic energy of the electron as well as a change in direction in the photon. The energy of the photon after interaction is defined as:

$$E' = \frac{E}{1 + \left(\frac{E}{m_0 c^2}\right)(1 - \cos\theta)} \quad (1.1)$$

where E is the energy of the incident photon, E' is the energy of the scattered photon, $m_0 c^2$ is the rest mass of the electron, and θ is the scattering angle [10]. From Equation 1.1, it can be seen that fairly large deflections can occur with just a small loss of energy; for example, for 511 keV photons, a Compton scattering event results in a deflection of over 25 degrees but results in just a 10% loss in the photon energy. Random coincidence is the simultaneous detection of emission from more than one decay event. It occurs when two photons not arising from the same annihilation event are incident on the detectors within the coincidence time-window of the system. This contributes to statistical noise in data as well as overestimation of isotope concentration [8].

Multiple coincidences occur when more than two photons are detected by different detectors within the coincidence resolving time. This type of event either causes event mis-positioning or rejection because it is not possible to determine the line of response to which the event should be assigned. Coincidence events are grouped together to produce projection images called sonograms. Acquisition of PET images is not a simple process because data corrections are required for scattered, random coincidences as well as for the effects of attenuation, because the data acquired from the PET camera are given as projections. The measured projections are different from the projections assumed in image reconstruction [9]. Reconstruction of images from projections is computationally burdensome. Data reconstruction and correction are usually carried out by analytical or iterative methods. Analytical methods are simple, fast, and usually have predictable linear behaviour. However, such methods are not very flexible and have problems associated with noise resolution and image properties and do not allow for quantitative imaging. On the other hand, iterative methods allow for quantitative imaging but require long calculation times as well as amplification of the background noise; it thus requires counts to be low to reduce the projection noise.

1.2.2 Advantages and Limitations

PET is a highly sensitive and popular technique in preclinical and clinical imaging. It is a very important diagnostic technique because disease processes such as cancer often begin with functional changes at the cellular level. There are many radioactive tracers with various half-lives applicable for different preclinical and clinical applications. The half-lives are often very short and therefore must be injected immediately after production. Due to the mechanism of decay being the same for all different radioactive tracers, it is only possible to trace one molecular species in a given imaging experiment or clinical scan where only true coincidence events are used.

Tracers can be designed to be target-specific to tumours and allow study of metabolic activities such as bone metabolism and bone metastasis that are common in a lot of cancers. Thus this technique can be used to monitor disease processes and patients' responses to therapy. However, one of the major limitations of PET is its poor spatial resolution. It is also limited by pixel sampling rate, quantity of the radioactive source, and blurring in the phosphor screens of the detector rings. However, the use of electronic collimation over physical collimation helps to improve sensitivity and uniformity of the emitting source response function.

1.3 WHAT IS SINGLE PHOTON EMISSION COMPUTED TOMOGRAPHY (SPECT)?

SPECT is another nuclear imaging technique for imaging molecules, metabolisms, and biochemical functions of organs and cells, and like PET, the use of radioisotopes is required. As its name suggests, it involves the emission of a single γ -ray per nuclear disintegration, which is measured directly, unlike in PET, where the positrons are emitted to produce the γ -rays. Numerous single γ -rays are detected by rotating gamma cameras to reconstruct an image of the origin of the γ -rays, which identifies the location of the radioisotope. Thus, specific radio-ligands are used to incorporate typical radioisotopes such as ^{99m}Tc to target to areas of interest [11]. An example of a radiopharmaceutical commonly used in cardiac imaging is ^{99m}Tc -tetrofosmin, also known as 'Myoview' (Figure 1.7) [12].

1.3.1 Basic Principles

Gamma rays from radioactive nuclides, apart from radioactive decay, also produce other forms of radiation such as alpha and beta. A gamma ray results from the relaxation of an excited daughter nucleus to a lower energy state after a nucleus emits an α or β particle [13]. An example of this is technetium-99, which is a commonly used radioisotope in radiopharmaceuticals produced from molybdenum-99. As shown in Figure 1.8, the excited nuclear state is more stable than average excited states after a β -decay where a β particle is released, thus the daughter nucleus forms a metastable excited state resulting in the

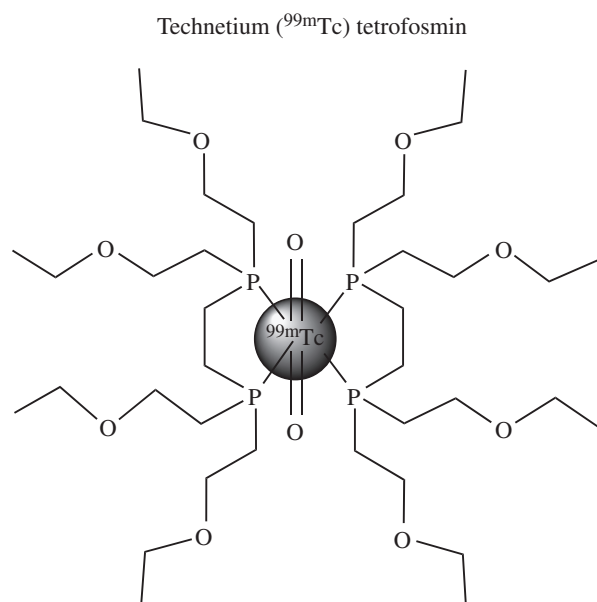


FIGURE 1.7 Myoview: A typical contrast agent used in SPECT.

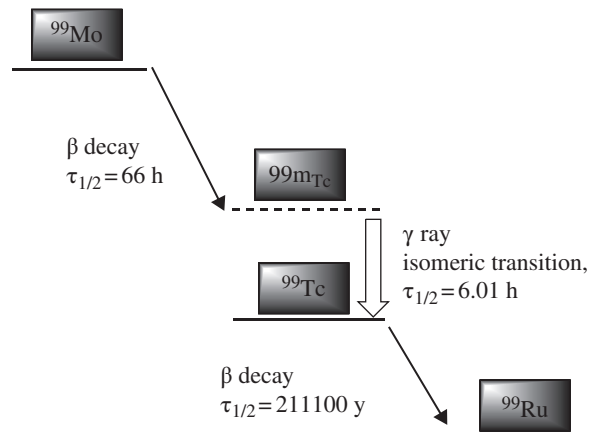


FIGURE 1.8 A schematic for the formation of ^{99m}Tc .

nuclear isomer, ^{99m}Tc . This isomer has a short half-life of ~ 6 hours before it goes to ^{99}Tc by isomeric transition, a radioactive decay process from an excited metastable state that results in γ -ray emission [13, 14].

In SPECT, these γ -ray emissions are detected by a 360° rotating photon detector array around the body known as the gamma camera, which can acquire multiple 3D projections at multiple angles. Sodium iodide or solid-state cadmium-zinc-telluride detectors, which provide spatial resolution of 1–2 mm, are usually used. Images are formed with the information given on the position and concentration of the radionuclide biodistribution in two dimensions [14]. However, due to the attenuation effects of γ -ray emission as it is transmitted from the injected tracers inside the body, mathematical reconstruction algorithms have been developed to improve resolution. Some other common radionuclides used in SPECT in addition to ^{99m}Tc are ^{111}In (half-life 2.8 days), ^{123}I (13.2 h), and ^{125}I (59.5 days). Due to the different half-lives, dual tracers can be used to give simultaneous imaging because the γ -ray emissions have different energies [14, 15].

A gamma detector is made up of a few cameras that are placed opposite to one another to form a cylindrical detector that allows rotation around an axis centre. Due to its multiple camera heads, it only needs to rotate 120–180 degrees to collect data around the entire body. The gamma camera is made up of three basic layers, the first of which contains a collimator, a special lens that only allows entry of γ -rays that are perpendicular to the plane of the camera. The other two layers consist of a crystal and detectors. The crystal is usually a thallium-activated sodium iodide [NaI(Tl)] detector crystal, which, when absorbing γ -rays, would scintillate to cause a light signal to be detected (Figure 1.9) [15].

The data are collected as a planar matrix of values that correspond to the number of gamma counts and can be processed to give planar scintigrams for constructing 2D images. Typically, each row across the matrix represents an intensity displayed across a single projection, whereas the successive rows represent successive projection angles. There are different techniques to reconstruct tomographic images that are different for 2D cross-sectional images and for 3D images. A common reconstruction method is the simple back-projection method, which generates 2D cross-sectional images of activity from a slice within the detected object, using the projection profiles obtained for that slice. However, there is a flaw in this method of data reconstruction: The final SPECT images have poorer spatial resolution than the raw 2D images used to produce them. For better spatial resolution, other processing techniques such as direct Fourier transform reconstruction as well as data filtering can be used. Filtered back-projection is a favourable method for data reconstruction. For tomographic 3D images, 3D reconstruction algorithms can also be used to visualise the 3D biodistribution of the radiotracers.

The resolution and sensitivity of SPECT is dependent on the pinhole of the collimator multiple-pinhole and multiple-solid state detector systems are often used to allow for lower radiation dosages and shorter scan times, hence improving the sensitivity and resolution of this imaging modality [16, 17].

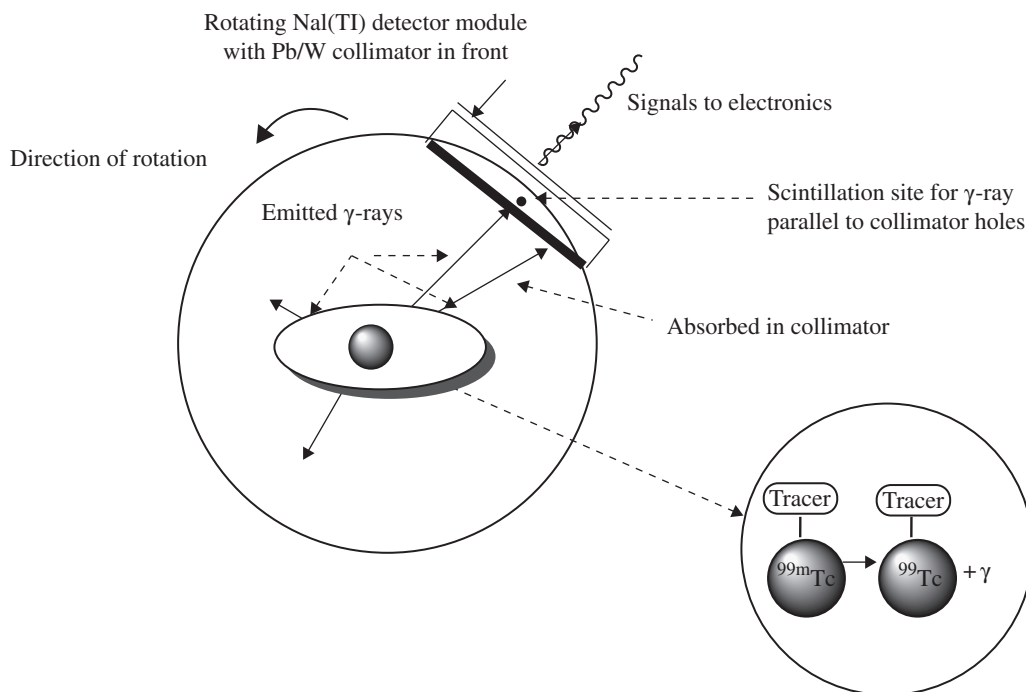


FIGURE 1.9 Schematic diagram showing the basic principles of SPECT.

1.3.2 Advantages and Limitations

One of the major advantages of SPECT over other imaging modalities is that it provides improved contrast between regions of different functions, thus allowing improved detection of abnormal physiological functions. SPECT also gives better spatial localisation as well as improved quantification. It offers greater accessibility because it uses radioisotopes with longer half-lives and, unlike PET, does not require any cyclotrons to generate these radioisotopes. Due to the selection of radioisotopes available, it allows simultaneous imaging because different radioisotopes produce different γ -rays of different energies (Table 1.1). This is a unique advantage of SPECT because multiple energy windows can be used for concurrent imaging of different functions and metabolic processes.

However, this technique also has disadvantages: It is often necessary to use long scanning times, which can cause discomfort to patients. Artefacts can also be easily generated by numerous uncontrollable factors such as patient movement and uneven distribution of the radiotracer.

1.4 WHAT IS COMPUTED TOMOGRAPHY (CT) OR COMPUTED AXIAL TOMOGRAPHY (CAT)?

Computed tomography (CT) or computed axial tomography (CAT) is a diagnostic technique that uses special X-ray equipment to obtain cross-sectional pictures of the body [18]. This technique allows detailed imaging of organs, bones, and tissues and is often used in conjunction with other diagnostic methods such as MRI and PET (Figure 1.10) [19].

1.4.1 Basic Principles

X-rays are a form of electromagnetic radiation with a wavelength in the range of 0.01 to 10 nm that can transverse along the cross-section of an object in straight lines. The wavelength is attenuated by the object through which it passes but is still detectable outside the object [20]. In CT imaging, the cross-section is probed with X-rays from various directions with the use of rotating X-ray equipment where both the low energy X-ray source and the detector are rotated at 360 degrees around the patient. The acquired attenuated signals are then recorded and converted into projections of the linear attenuation coefficient distribution of the cross-section to produce volumetric data. Charged Coupled Device (CCD) detectors are used to carry out photo-transduction of incoming X-rays to produce images. The contrast in CT images relies on the

TABLE 1.1 Types of Radioisotopes Used for Different Studies by SPECT Imaging.

Study	Radioisotope	Emission energy (keV)	Half-life	Radiopharmaceutical	Activity (MBq)
Bone scan	technetium-99 m	140	6 hours	Phosphonates / Bisphosphonates	800
Myocardial perfusion scan	technetium-99 m	140	6 hours	tetrofosmin; Sestamibi	700
Brain scan	technetium-99 m	140	6 hours	HMPAO; ECD	555–1110
Tumour scan	iodine-123	159	13 hours	MIBG	400
White cell scan	indium-111 & technetium-99 m	171 & 245	67 hours	<i>in vitro</i> labelled leucocytes	18

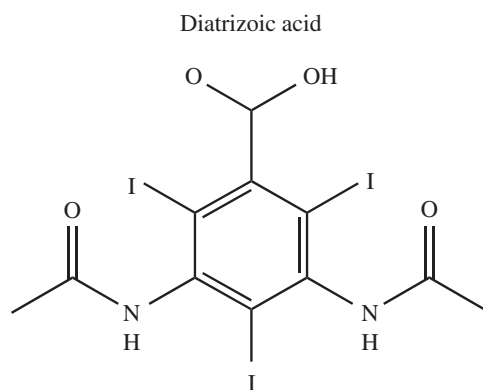


FIGURE 1.10 A typical contrast agent used in CT-Gastrografin.

intrinsic structural and absorption differences in the properties through which the X-rays travel, such as tissues, organs, bone, fat, water, and air [20].

In CT imaging, cross-sectional images of body organs and tissues are obtained at very high resolution, thus allowing differentiation among different types of tissue. The images are reconstructed from computers using the Fourier transform, a mathematical operation that reconstructs the cross-section to form an image of a slice through the body with the focal point centred at the position of the X-ray beam. This is the most basic image that can be obtained. Other more advanced image reconstruction, such as 3D images, can also be produced by taking multiple scans at short intervals and then stacking the slices together. Dynamic spatial reconstruction (DSR) is also possible by using approximately 30 X-ray tubes to produce images that show changes through time; thus, dynamic changes in structure and function can be monitored [20, 21]. CT imaging can provide views of soft tissue, bone, muscle, and blood vessels without compromising clarity. Other imaging techniques are much more limited in the types of images they can provide, so CT is commonly used for diagnostic purposes [21]. With the use of contrast agents such as iodinated contrast agents, imaging of tumours is also possible, providing information on size and localisation, thus aiding planning in treatment, whether for surgery or radiotherapy.

The use of higher energy X-rays can also improve resolution but can be problematic especially in the health of human patients because it increases ionizing radiation damage. Normally, higher X-ray CT machines are used for animal studies. As mentioned previously, CT images are generated by creating slices through the body; this is recorded as areas of varying CT intensities and represented in pixels. These pixels are represented by a number that is quantitative to the amount of X-ray beam absorbed by the tissues at each individual point in the body.

The image is created according to the density of the tissue from a matrix of pixels that are converted to CT numbers known as Hounsfield numbers (HU, Eq. 1.2). This scale is defined in Hounsfield units (HU) and shown in Figure 1.11. The denser the tissues are, the higher the value of the numbers, thus a greyscale is created. Different windows and levels are created from these numbers to produce an image. Different size windows affect the quality of the image by defining the range as well as the upper and lower limits. For example, a large window shows the major structures, whereas a small window shows finer details that are often used to discern tissues of similar density. The Hounsfield number at the centre of the window is referenced at the level and is used to define the range for the window associated with the type of structure of interest. To enhance CT images, high density contrast agents as well as multi-slice detector geometries that allow whole-body imaging are used; these help to reduce scanning times and patient discomfort as well as artefacts.

$$HU = \frac{\mu_X - \mu_{\text{Water}}}{\mu_{\text{Water}} - \mu_{\text{Air}}} \times 1000 \quad (1.2)$$

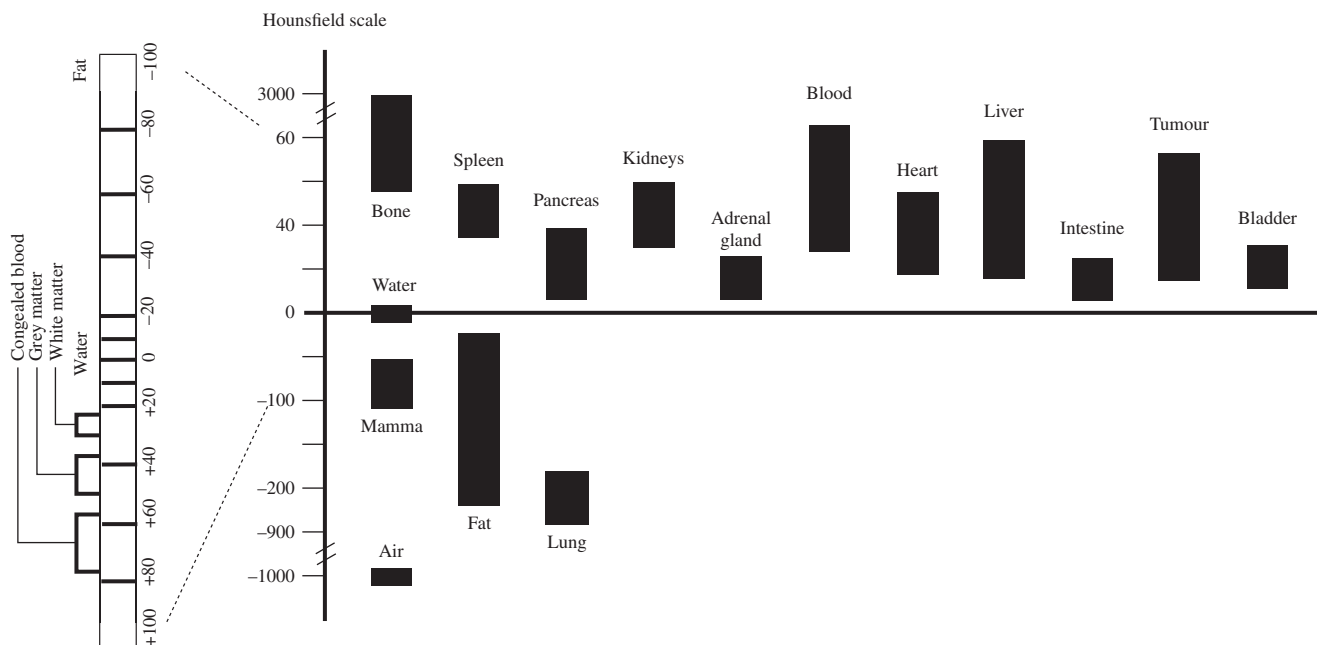


FIGURE 1.11 The Hounsfield Scale and the equation for the Hounsfield Unit (Eq. 1.2).

1.4.2 Advantages and Limitations

CT imaging provides fast and high spatial resolution images that allow fine visualization of anatomical details. As a diagnostic technique, it is often used to detect or confirm cancerous tumours by providing detailed information such as the size and location of the tumour to help planning for radiation therapy or surgery. One of the major advantages of CT is that it could be combined with other imaging modalities such as PET and MRI to provide other information such as dynamic and metabolic data (Figure 1.12). However, repeated CT imaging carries health risks to the patient due to exposure to non-negligible radiation dosage.

Another problem is that the scanning procedure can be quite time-consuming and may require up to an hour to complete. This could cause discomfort to patients in some cases. In general, CT imaging is a pain-free procedure, and it is often incorporated into other techniques to create powerful multimodal imaging modalities to give improved sensitivity and resolution for diagnosis, especially in cancer. The improvement in images due to the use of combined techniques such as CT and PET are shown in Figure 1.13. It is apparent that the combined use of CT and PET provides more information on tumours, such as their location and size as well as growth and metabolic activity of tissues [23].

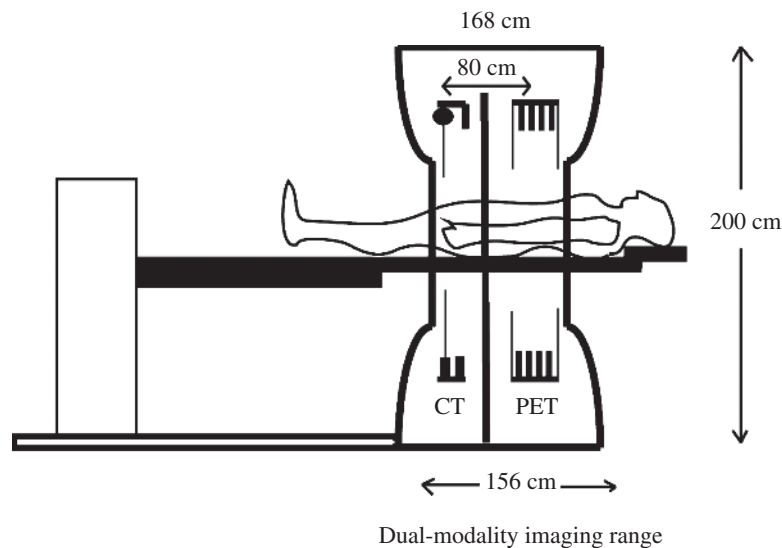


FIGURE 1.12 Diagram showing a typical CT-PET instrument [22].

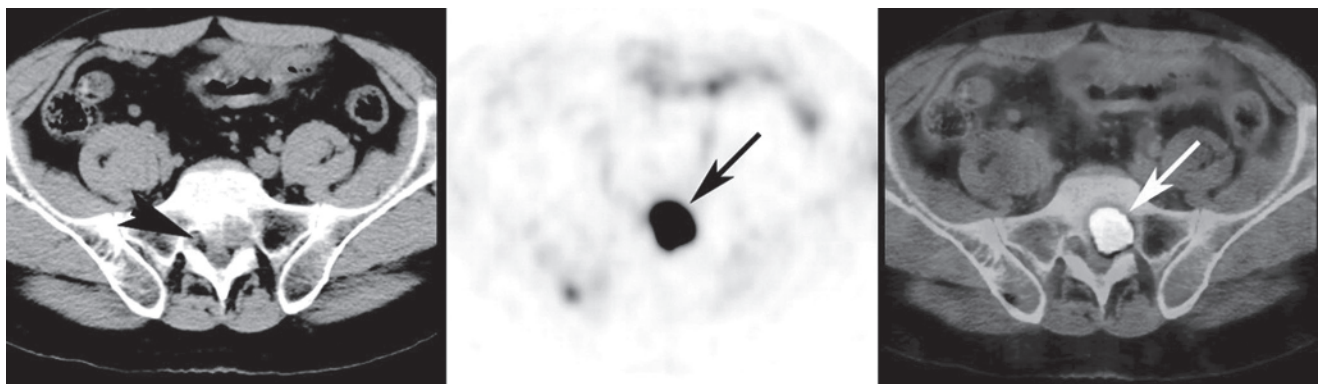


FIGURE 1.13 Left: Image from a CT scan; Middle: Image from a PET scan; Right: Image from a CT-PET scan [23]. (See insert for colour representation of the figure.)

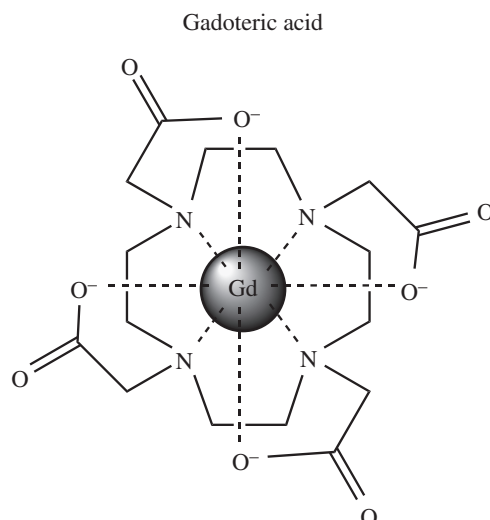


FIGURE 1.14 Dotarem: A typical contrast agent used in MRI.

1.5 WHAT IS MAGNETIC RESONANCE IMAGING (MRI)?

Magnetic resonance imaging (MRI) is an imaging technique based on the principles of nuclear magnetic resonance (NMR), which provides microscopic chemical and physical information about molecules. Instead of obtaining information about chemical shifts and coupling constants, MRI gives spatial distribution of the intensity of water proton signals in the body [24]. MRI measures the relaxation of free hydrogen nuclei when they realign to their original state in the direction of the magnetic field after having been excited by a radio frequency (Rf). Different image contrasts can be achieved by using different pulse sequences or by changing the imaging parameters such as longitudinal relaxation time (T_1) and transverse relaxation time (T_2). Contrast agents are also used to improve the quality of the image (Figure 1.14) [25].

1.5.1 Basic Principles

Approximately 63% of the human body is primarily fat and water, which are comprised of many hydrogen atoms. Thus, MRI focuses mostly on NMR signals from hydrogen nuclei. Nuclei are charged particles that have characteristic motion or precession that produces a small magnetic moment. In the presence of a magnetic field, the nuclei would move about it in a phenomenon known as the Larmor precession. The frequency of Larmor precession is proportional to the applied magnetic field strength as defined by the Larmor frequency ω_0 , $\Rightarrow \omega_0 = \gamma B_0$, where γ is the gyromagnetic ratio and B_0 is the strength of the applied magnetic field. The gyromagnetic ratio is a nuclei-specific constant, for hydrogen, $\gamma = 42.6 \text{ MHz/Tesla}$. A strong uniform magnetic field of 1.5 or 3 Tesla is generally used in a typical human scanner [24–26]. MRI measures the relaxation of free hydrogen nuclei after they have been excited by a radio frequency. The electric field of the radio frequency creates a new magnetic field, B_1 , which induces protons away from the original field, B_0 . The nuclei spins acquire enough energy to tilt/flip and precess. This ‘flip’ is time- and power-dependent on the B_1 field and hence the RF pulse. When the RF field is off, the protons are able to realign to their original state in the direction of the magnetic field, B_0 , by T_1 and T_2 relaxation. In a strong magnetic field, the hydrogen nuclei spin is aligned in a direction parallel to the field. This process is illustrated in Figure 1.15.

The signal recorded in MRI is the energy given or lost after relaxation of the nuclei from the RF excitation. This signal is the “spin echo,” which is composed of multiple frequencies, reflecting different positions along the magnetic field gradient. Fourier transform is used to process these frequencies where the magnitude of the signal at each frequency is proportional to the hydrogen density at that location, thus allowing images to be constructed. Hence, spatial information in MRI is encoded in the frequency of the signal, which is dependent on the local value of the magnetic field. The generation of MRI images requires the combination of both spatial and intensity information. The signal intensity is mostly affected by the T_1 and T_2 relaxation parameters. although in general, the overall quality of the image is strongly dependent on hardware design such as the transmitting and receiving coil design.

In order to understand how the contrasts of the images are generated, it is important to note that each proton has a unique T_1 and T_2 , which are parameters that can be easily altered [27–29]. Proton relaxation is a process of realigning

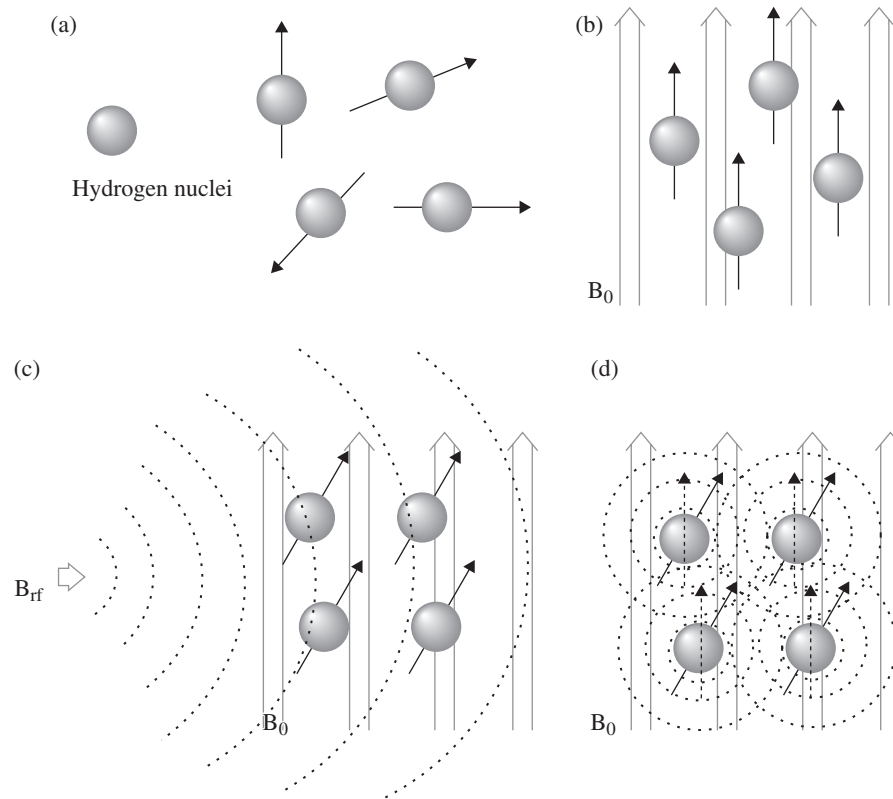


FIGURE 1.15 (a) Hydrogen nuclei are randomly aligned in the absence of any strong magnetic fields. (b) All hydrogen nuclei, in the presence of a strong magnetic field B_0 , are aligned in parallel with the magnetic field to create a net magnetic moment, M , which is parallel to B_0 . (c) A radio-frequency pulse B_{rf} is applied perpendicularly to the magnetic field B_0 . This pulse, with a frequency equal to the Larmor frequency, causes the net magnetic moment of the nuclei M to tilt away from B_0 . (d) The RF pulse stops and the net momentum of the nuclei realigns back in parallel to B_0 by relaxation, at the same time the nuclei lose energy to give an RF signal.

with B_0 . There are two different types of relaxation, T_1 and T_2 , the longitudinal relaxation time and the transverse relaxation time respectively. The T_1 and T_2 relaxation times define the way the protons revert back to their resting states after the initial RF pulse. As protons relax, they realign along B_0 by T_1 where T_1 is the recovery of magnetisation along the longitudinal axis. They also lose phase coherence by T_2 , which is the decay of magnetisation along the transverse axis. These two parameters are the most significant in providing image contrast in MRI. The time constant of T_1 is tissue-dependent. Signal strength decreases in time with a loss of phase coherence of the spins. This decrease occurs at a time constant T_2 , which is always less than T_1 (Figure 1.16). During T_1 and T_2 relaxation, the nuclei lose energy by emitting their own RF signals; however, only transverse magnetisation produces a signal. This signal is referred to as the free-induction decay (FID) response signal. The FID response signal is measured by a conductive field coil placed around the object being imaged, and the FID decays at a rate given by the tissue relaxation parameter known as T_2^* . The measurement of the FID signal gives images that have different weightings depending on the T_1 , T_2 , and T_2^* . These signals are processed or reconstructed to obtain greyscale contrast 3D images [24]. The different properties between T_1 and T_2 are shown in Table 1.2.

Although the human body contains a high percentage of water, the signal intensity is not just dependent on the amount of water at the location, and experimentally it is hard to change the proton density in tissue to look at small changes. Thus, chemical contrast agents are used to change the characteristics of tissue by altering the magnetic relaxation times of T_1 and T_2 , which normally amplifies the contrast, and these agents are classed as T_1 and T_2 agents.

Ferromagnetic contrast agents alter the contrast by changing the T_2^* of the water molecules around the ferromagnetic contrast agent by distorting the B_0 magnetic field around the ferromagnetic material in the contrast agent. These contrast agents are typically iron nanoparticles with bio-organic compatible substrates. Paramagnetic contrast agents, which are much more commonly used, alter the contrast by producing time-varying magnetic fields that promote T_1 relaxation of water molecules. The time-varying magnetic fields come from both rotational motion of the contrast agent and electron spin flips associated with the unpaired electrons in the paramagnetic material in the contrast agent. This is why gadolinium agents are the most favourable because the f-element Gd ion has the maximum seven unpaired electrons [29].

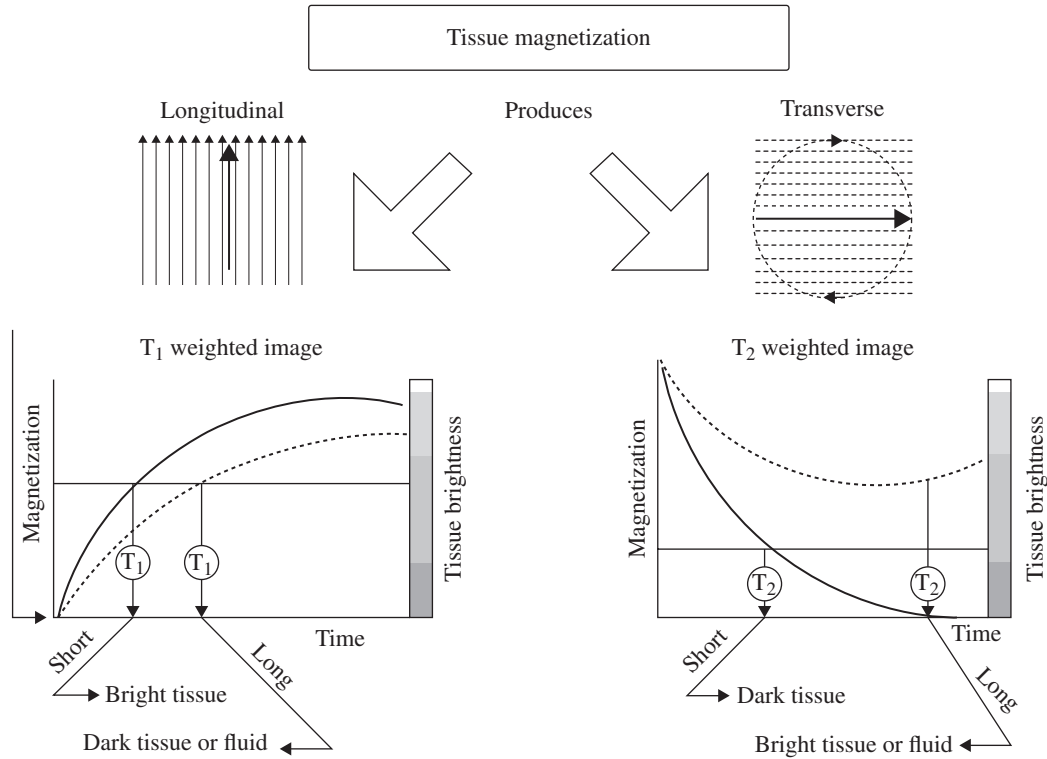


FIGURE 1.16 Comparison of T_1 and T_2 properties.

TABLE 1.2 Properties of T_1 and T_2 Relaxation.

T_1 is called the “spin-lattice” relaxation time	T_2 is called the “spin-spin” relaxation time
Recovery of magnetisation along the longitudinal axis: longitudinal relaxation time	Decay of magnetisation along the transverse axis: transverse relaxation time
Measurement of the “lattice” around the spin	Measurement of the “spins” around the spin
Rotational correlation time “ τ_r ” $\sim 1/T_1$	Translational correlation “ τ_c ” $\sim 1/T_2$
Time to rotate one radian (10–12 sec)	Time to diffuse one diameter (10–11 sec)
$= (4\pi) \eta a^3 / 3kT$, where a is radius, η is viscosity	$= (6\pi) \eta D / kT$, where D is diffusion, η is viscosity
Free protons rotate rapidly and have short τ_r	Free protons move rapidly and have short τ_c . This is observed as a long T_2 .
This is observed as a long T_1 .	Hindered protons move slowly and have long τ_c . This translates into a short T_2 .
Bound protons hit barriers and have long τ_r . This translates into a short T_1 .	

T_1 and T_2 may be shortened considerably in the presence of a paramagnetic contrast agent. However, a compromise is necessary because the shortening of T_1 would lead to an increase in signal intensity, while the shortening of T_2 would produce broader lines with decreased intensity. This reflects a nonlinear relationship between signal intensity and concentration of the contrast agent. At low concentrations, an increase in the concentration of the contrast agent would cause an increase in signal intensity until the optimal concentration is reached due to effects on T_1 . Further increase in the concentration would reduce the intensity of the signal because of the effects on T_2 . The relationship between T_1 and T_2 dictates the design of contrast agents, which must have a relatively greater effect on T_1 than on T_2 , as well as the use of pulse sequences that emphasise changes in T_1 .

Gadolinium-based contrast agents are usually used in MRI because of their excellent paramagnetic properties and biological tolerance. However, there are some concerns regarding the problem of toxicity. Problems are related to transmetallation, which is the exchange of the metal in the contrast agent with a metal ion in solution (Eq. 1.3) [28].



Toxicity, specificity, and relaxivity are three important criteria in the design of contrast agents. Many of these paramagnetic metals are toxic as free ions. Thus, the design and study of contrast agents is very important in MRI because these

agents are injected in large doses especially compared with the quantities used in nuclear imaging techniques. For example, Gd-based contrast agents are injected intravenously at a dosage of 0.1 mmol/kg. Relaxivity is the ability of a magnetic contrast agent to increase the relaxation rates of the surrounding water proton spins, which depends on the molecular structure and kinetics of the complex. The relaxivity (r_1 or r_2) of a contrast agent in water is the change in $1/T_1$ or $1/T_2$ of water per concentration of contrast agent and is dependent on parameters such as temperature and magnetic field. The relationship between T_1 , r_1 , and the concentration of the paramagnetic material is given in Equation (1.4) where M is a magnetic ion [29].

$$1/T_{1(\text{Measured})} = 1/T_{1(\text{Water})} + r_1[M] \quad (1.4)$$

Because most T_1 contrast agents are unable to cross the intact blood-brain barrier, they are not used for brain imaging. Studies have shown that T_2 -weighted imaging is more sensitive for detecting brain pathology as well as for imaging edema. However, the use of functional MRI (fMRI), a branch of the MRI modality, is more commonly used to measure brain activity in response to specified stimuli. This technique allows study of the functions of the living brain in a noninvasive manner and is clinically used in the treatment of brain tumours [29].

1.5.2 Advantages and Limitations

MRI provides excellent tissue contrast and higher spatial resolution and is one of the best techniques for showing anatomical detail. It is very useful in early-stage diagnosis of diseases, especially for brain tumours, and in providing information on the biochemistry and metabolism of tissues. It does not require any ionising radiation, and simultaneous extraction of physiologic and anatomic information is possible. Spatial resolution can be increased by increasing the acquisition time without endangering patients, compared with radioisotope imaging techniques. fMRI allows non-invasive imaging of the brain without the use of any external contrast agents, but the images are of lower spatial resolution. Advances in technology design allows for a smaller receiver coil radius and high magnetic field strengths to improve signal to noise ratio and resolution. However, this gives rise to other technical challenges, such as artefacts and problems of physiological effects on human patients. Figure 1.17 schematically shows the basics of an MRI machine.

In terms of disadvantages, MRI is several orders of magnitude less sensitive than nuclear imaging modalities because only a small percentage of protons are able to absorb the radiofrequency energy to generate a data signal. Reliable signal amplification strategies as well as good contrast agents are thus required. A good contrast agent can improve the sensitivity of the signals because it alters the relaxation times of tissues in the area but only in regions in which the contrast agents are concentrated. MRI also requires a much larger dosage of contrast agents than, for example, radiotracers in nuclear imaging, making toxicity of the imaging agents a major area of concern in molecular design and development. Rigorous tests and clinical trials are thus required in order for MRI contrast agents to be approved by the FDA.

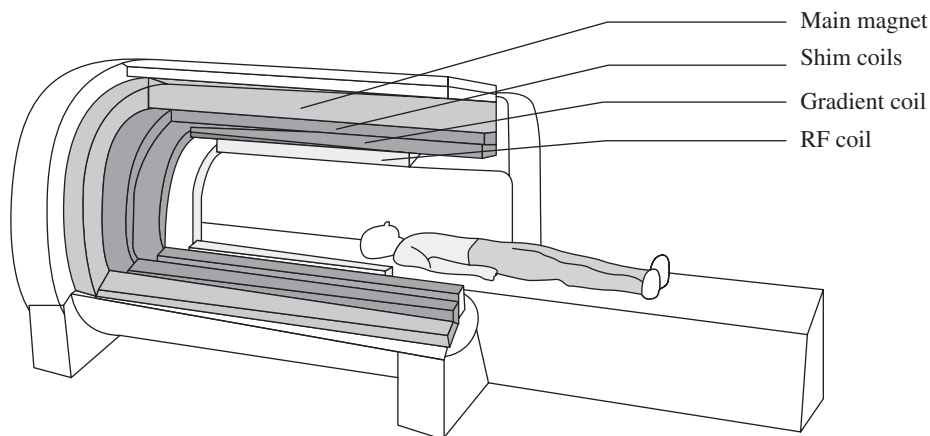


FIGURE 1.17 Components of a typical MRI scanner.

1.6 WHAT IS OPTICAL IMAGING?

Optical imaging techniques exploit different properties of light, such as absorption, emission, reflectance, scattering, polarisation, coherence, and fluorescence, as a source of contrast. Such contrast is created by the interaction of photons with different tissue or cellular components. Fluorescent and luminescent properties of light are generally used in *in vivo* studies. Therefore, this section will focus on fluorescence imaging. Although other optical imaging systems such as bioluminescence imaging, optical coherence tomography, photoacoustic microscopy, and tissue spectroscopy are not mentioned here (but are briefly discussed in Chapter 11), this does not mean that they play a less significant role in the development of optical imaging.

Fluorescence-based techniques are extremely valuable for studying cellular structures, functions, and pathways as well as molecular interactions in biological systems. These techniques utilise microscopy systems to observe and image at the microscopic and macroscopic levels, as well as molecular labels/dyes for contrast enhancement [30]. There are numerous types of labels and dyes for optical imaging; one example of a classic dye is shown in Figure 1.18.

1.6.1 Basic Principles

Fluorescence results from a process that occurs when certain molecules absorb light. These molecules are generally polyaromatic hydrocarbons or heterocycles known as fluorophores. They absorb energy at a particular wavelength and emit energy at a different but specific wavelength. This can be explained by a simple electronic state Jablonski diagram (Figure 1.19).

The electronic states of most organic molecules are either singlet states (S_1), when all electrons in the molecule are spin-paired, or triplet states (T_1), when one set of electron spins is unpaired. Upon excitation, the molecules move to a temporary excited state S_1 , which can relax by numerous decay mechanisms to go back to its original ground state S_0 . There are numerous decay processes; the two important types are nonradiative decay, where energy is lost by vibronic motions, or by radiative decay, in which energy is lost by fluorescence. Fluorescence is an important property that is manipulated in fluorescence microscopy. It can be quantified by monitoring the emission quantum yield and the emission lifetime (decay), which dictate the selection criteria for designing fluorophores. The fluorescence quantum efficiency of a fluorophore is the ratio of fluorescence photons emitted to the photons absorbed [31]. It is given as a quantum yield percentage where the quantum efficiency of emission is calculated using standard samples (which have a fixed and known fluorescence quantum yield value) according to Equation (1.5) [32]:

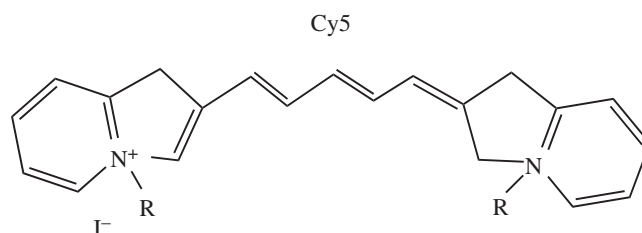


FIGURE 1.18 Cy5, a typical dye used in optical imaging.

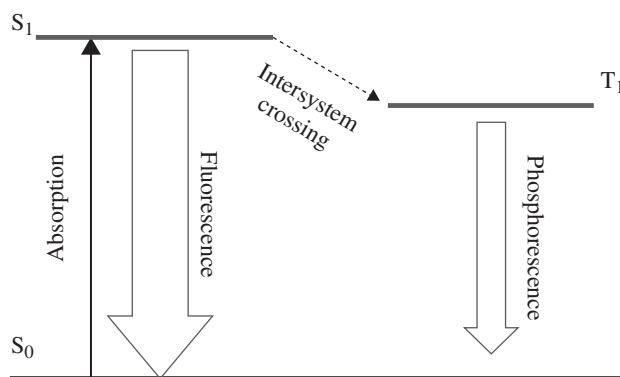


FIGURE 1.19 Jablonski diagram showing the basic principles of fluorescence.

$$\Phi_x = \Phi_{ST} [A_x / A_{ST}] [\eta_x^2 / \eta_{ST}^2] \quad (1.5)$$

where the subscripts ST and X denote standard and samples respectively, Φ is the fluorescence quantum yield, A the integrated area of emission band, and η the refractive index of the solvent. Φ can be used to assess the brightness of the fluorophore, which is the product of the quantum yield and the extinction coefficient of the fluorophore.

The advent of traditional fluorescence microscopy has initiated an important era in the study of living cells. Since then, many more creative engineering and sophisticated designs of microscopes have emerged, providing new and better optical imaging techniques for both academic and clinical studies. Simultaneously, it has also given rise to a new research area in the development of biological fluorophores, such as fluorescent proteins and GFP, which have provided insight into cellular structures and functions. Fluorophores improve or define image contrast, which is the difference between the highest and

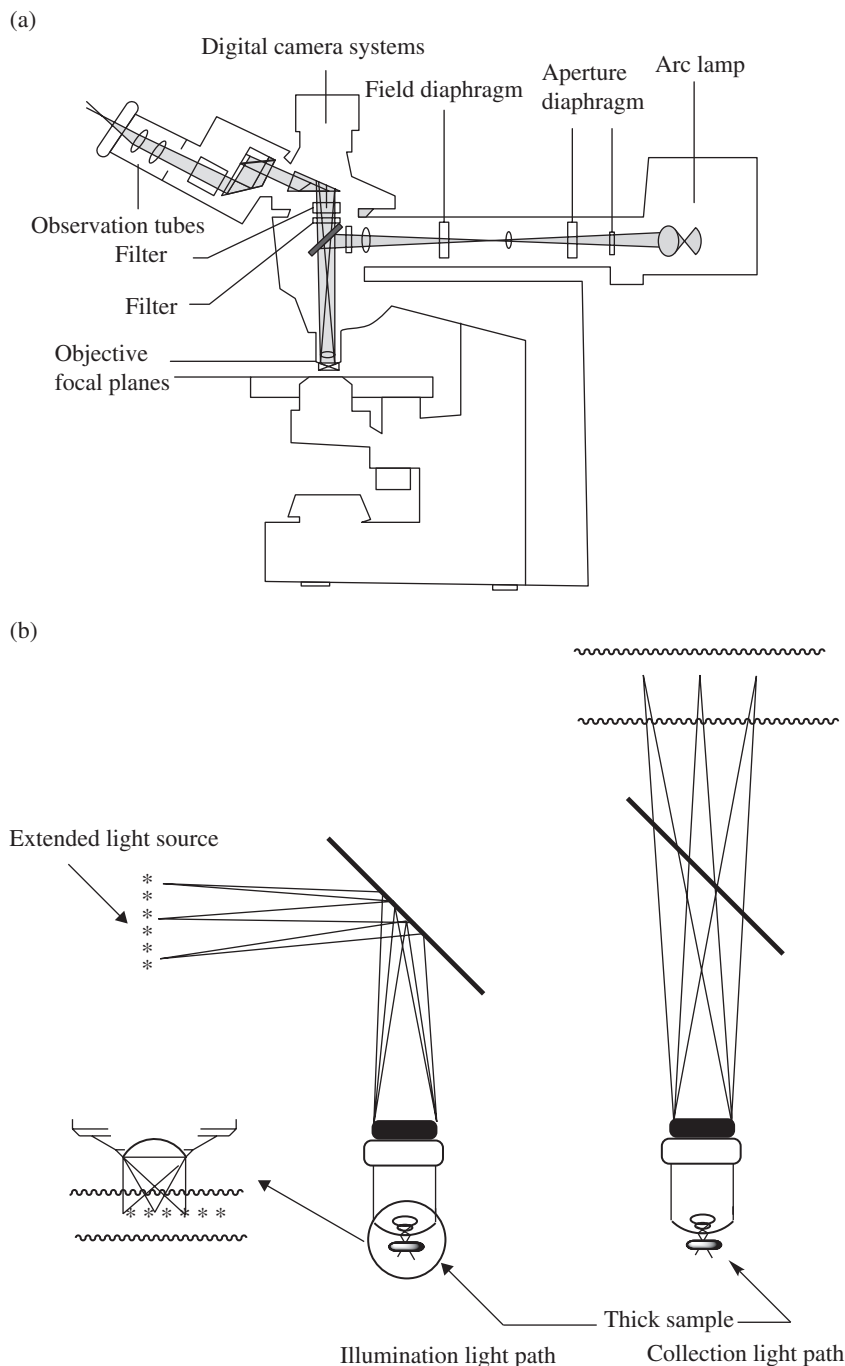


FIGURE 1.20 (a) A conventional fluorescence microscope and (b) the light path in a fluorescence microscope.

lowest signal intensity of two points in an image. This is important because without contrast, signal differences between background and the resolution of the optical lens cannot be differentiated [33]. All fluorescence imaging systems consist of the following key elements: excitation source; light delivery optics such as mirror; light collection and filtration optics; and light detection, amplification, and digitisation systems. There are numerous types of fluorescence microscope systems available; however, only two of the simplest and most common microscopes, conventional and confocal, will be discussed.

1.6.2 Conventional or Wide-Field Fluorescence Microscopy

In conventional fluorescence microscopy, also known as wide-field fluorescence microscopy, the excitation source excites the entire sample, which is lit up laterally and vertically (Figure 1.20). This causes interference and produces stray light, which decreases the resolution of the image. The excitation source is usually a mercury lamp that gives a window of various wavelengths at various intensities, the strongest excitation wavelengths being in the UV region, which are unsuitable for *in vivo* excitation. The window is quite broad, ranging from the UV to the visible red regions. Emission filters are necessary for wavelength selection.

Because of the mercury lamp excitation source, it is generally advantageous for imaging probes to have high molar extinction coefficients and high quantum yielding, especially for excitation in the continuous window between 450–540 nm where there is much lower intensity [34].

1.6.3 Confocal Microscopy or Confocal Laser Scanning Microscopy

In contrast, confocal microscopy uses point illumination where only a part or a point of the sample is excited at any one time. This technique utilises a pinhole in an optically conjugate plane in front of the detector to eliminate out-of-focus information and produce better quality images compared with wide-field images. In theory, only light from the focused focal plane reaches the detector. This is due to the attenuation of the light intensity, which rapidly falls off above and below the plane of focus as the beam converges and diverges. This reduces excitation of things that are out of the focal plane, hence eliminating a lot of unwanted background signals because these are deflected. Any out-of-focus light that enters the photo-detector normally has intensity that is too weak to be detected. Moreover, any point of light that is in the focal plane but not at the focal point will be blocked by the pinhole screen. This method, illustrated in Figure 1.21, is known as optical sectioning. Optical sectioning is affected by the size of the pinhole: The smaller the pinhole, the thinner the slice would become; but this is not definite because there are other influencing factors such as the wavelength of the light, numerical aperture of the lens, as well as reflecting index of the medium.

Three-dimensional images can be made from scanning many thin sections through the sample to create numerous optical sections that can be stacked together to produce an image. All these properties enable confocal microscopes to obtain better resolution. Generally, to obtain higher resolution images, a laser is used as the excitation source because it provides discrete wavelengths with very high intensities as well as a point light source of illumination. Depending on the laser system used, the desired wavelength can be selected, enabling a wider range of fluorophore probes/labels to be utilised [35–36].

By using laser sources, near-infrared fluorescence imaging is also possible. This is a less well developed technique that allows for deeper tissue imaging because at the excitation region of 650–900 nm, it allows for maximal tissue penetration but minimal autofluorescence. The near infrared region is also the region with the lowest absorption for haemoglobin, which is found in the blood and is responsible for absorbing the majority of visible light [37]. Optical imaging helps to increase the knowledge of entire biological pathways and accelerate a systems-wide understanding of biological complexity. In optical imaging high-affinity imaging agents/labels with appropriate pharmacokinetics are essential for imaging at the molecular level. This is because it is almost impossible to distinguish all cells, regardless of whether they are cancerous, from one another by *in vivo* imaging without labelling. There are numerous commercially available fluorescent labels to enhance the quality of optical imaging. These can be broadly categorised into genetic reporters, injectable imaging agents, and exogenous cell trackers [36–39].

1.6.4 Advantages and Limitations

The advantages and disadvantages of optical imaging methods are summarised in Table 1.3.

Although optical imaging methods are highly sensitive and relatively low cost, they have low spatial resolution (~1 mm) and poor depth penetration that is limited to several millimetres of tissues. Studies have shown that there is a 10-fold loss in photon intensity for every centimetre of tissue depth that the light penetrates, which leads to problems in signal quantification. Other typical problems are associated with absorption and light scattering. Thus, the biggest problem and challenge remains in manipulating this technique so that it can be used for opaque animal and hence, human studies. Sophisticated designs in microscopy and the use of different wavelength excitation sources, such as near infrared, have partially ameliorated this technique. Yet there are still too many limitations for it to be useful for clinical purposes, although it has been increasingly used for *in vivo* mechanistic and cellular studies.

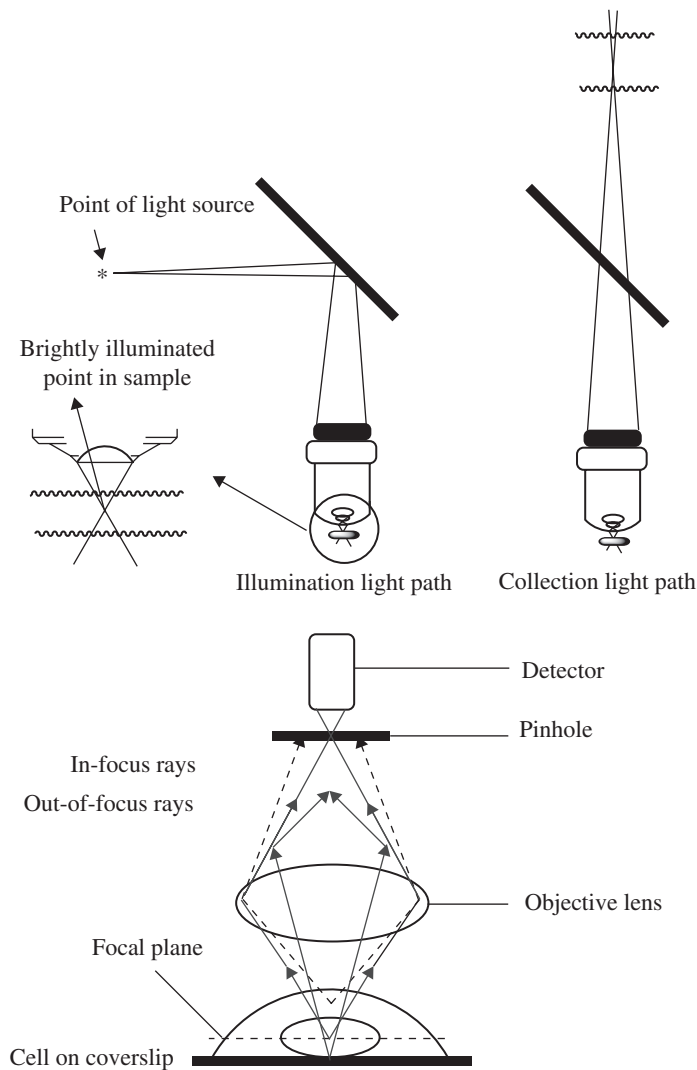


FIGURE 1.21 The light path in a confocal microscope.

TABLE 1.3 Different Types of Optical Imaging Methods.

Imaging Methods	Maximum Depth	Target	Time	Primary Small Animal Use	Clinical Potential
Confocal microscopy	300 μm	Physiological, Molecular	Sec/Min	Gene expression, reporter enzyme targeting, high sensitivity, and use in quantitative translational research	Experimental
Two-photon microscopy	800 μm	Physiological, Molecular	Sec/Min	Gene expression imaging, multiple probes simultaneously	Experimental
Fluorescence reflectance imaging	5–7 mm	Physiological, Molecular	Sec/Min	Gene expression activatable, detects fluorochromes in live and dead cells	Yes
Diffuse optical tomography	15–20 mm	Physiological, Molecular	Sec		Yes
Fluorescence molecular tomography	0–15 cm	Physiological, Molecular	Sec	Quantitative imaging of targeted fluorochrome reporters in deep tissues	No
Bioluminescence imaging	2–3 cm	Molecular	Min	Gene expression, cell tracking, quick and easy	Experimental

1.7 WHAT IS ULTRASOUND (US)?

Ultrasound waves are longitudinal sound waves that oscillate back and forth. Sound waves travel at a fixed velocity and oscillate by compression and decompression of the medium through which they are travelling or transmitting [40]. In US imaging, sound waves are emitted as pulses that are partly reflected and transmitted from a boundary between two tissue structures and are detected as echoes. The reflections of these waves are dependent on the different acoustical impedance between the two tissues: The larger the difference is, the stronger the signal of the echo would be. The echo is caused by the depth of the tissue interface and is the measured time response for the echo to travel back (Figure 1.22) [42, 43].

1.7.1 Basic Principles

The ultrasound used in diagnostic applications has frequencies (1–12MHz) higher than typical human hearing frequency ranges (15 000 ~ 20 000Hz) [43]. Unlike sound waves with lower frequencies that could diffract around corners, ultrasound travels more in a straight line, like electromagnetic light beams, and thus will be reflected. They are however, still longitudinal waves (Figure 1.23).

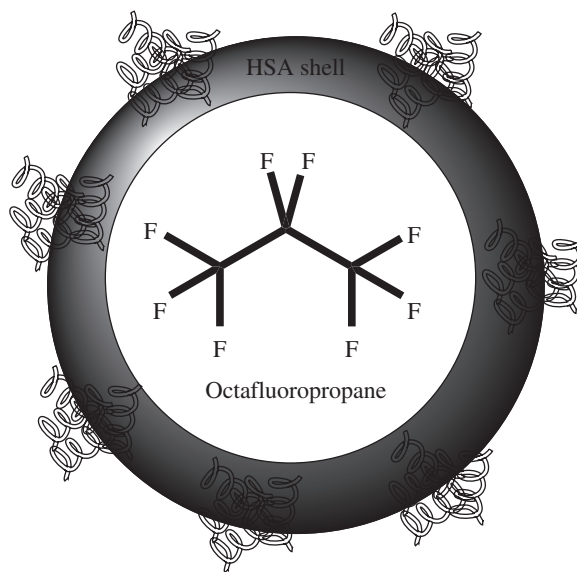


FIGURE 1.22 Microbubble, a typical contrast agent used in US.

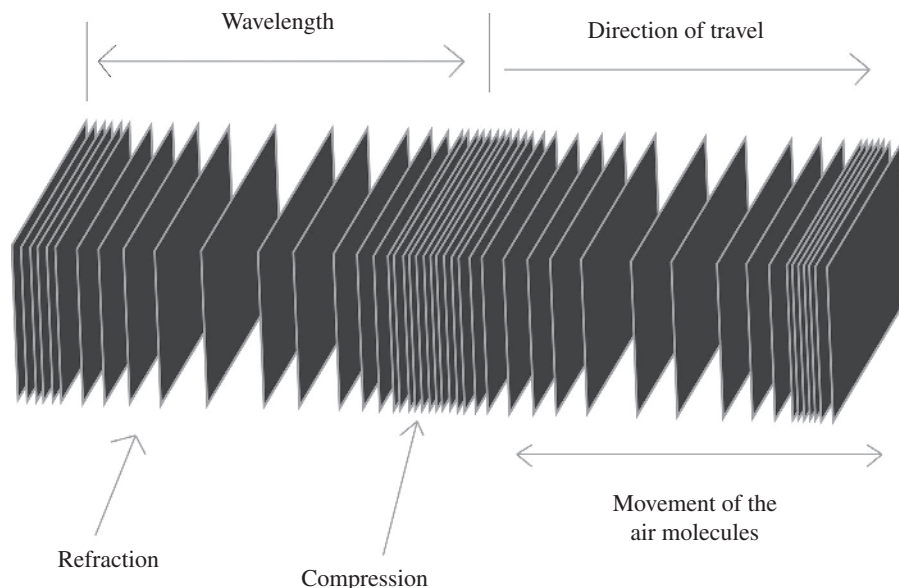


FIGURE 1.23 Basic properties of sound waves.

Because of this property, such waves can be used in diagnostic applications where they will be reflected by small objects. Yet it is also for this reason that US does not penetrate very deeply; this is a serious limitation for an imaging tool. Some general properties of sound waves will be mentioned briefly before discussing the use of US in imaging [44]. Wavelength λ is inversely related to the frequency f by the sound velocity c : Thus the velocity equals the wavelength times the number of oscillations per second (Eq. 1.6).

$$\lambda = c / f \Rightarrow c = \lambda f \quad (1.6)$$

Therefore, at a given temperature in a given material/medium, sound velocity is constant. Sound velocity varies due to the medium/material through which it is transmitting, and it is this property that is utilised in US imaging. This also means that simple gaseous media are problematic, because the sound waves cannot propagate easily through the medium. Therefore, ultrasound is unsuitable for imaging certain parts of the body, for example, the bowel, which is filled with air and organs that are obscured by the bowel. In general ultrasound imaging, only amplitude information is used in the reflected signal generated by an alternating current applied across piezoelectric crystals. These crystals are used in ultrasound probes to generate echoing signals to produce vibrations by compression and decompression. They also act as receiver of the reflected ultrasound. In ultrasound imaging, millions of pulses and echoes are transmitted and received every second. For each pulse emitted, the reflected signal is sampled multiple times. Different tissue structures reflect different amounts of emitted energy to produce signals with different amplitudes caused by the different depths of the structures. There are two different types of amplitudes: those from the transmitting pulses and those of the incoming pulses or signals that are a result of reflections produced from the sound waves hitting a surface structure. The energy of the amplitude of the reflected signals, as well as the incident, is known as the reflection coefficient, whereas the energy of the amplitude of the incident pulse and the transmitted pulse are called the transmission coefficient. These signals are affected by the difference in acoustic impedance of the different materials they are travelling through. The acoustic impedance of a medium is given by the equation $Z = c \times \rho$ and is defined as the speed of sound in a material \times the density [45].

When ultrasound signals hit a surface, not all the signals are reflected directly back to the transmitter; often many are lost due to scattering via the nature of the reflecting surface. When ultrasound is scattered in multiple directions, the reflecting surfaces are known as scatterers. There are two types of scatterers: irregular and regular. These are dependent on the types of surfaces that the sound waves are subjected to (Figure 1.24). An irregular scatterer reflects only a small portion of the incoming sound wave back to the detecting probe. A regular scatterer reflects a larger portion of the sound waves back and is caused by reflecting surfaces that are perpendicular to the ultrasound beam. In general, the reflecting surface affects the

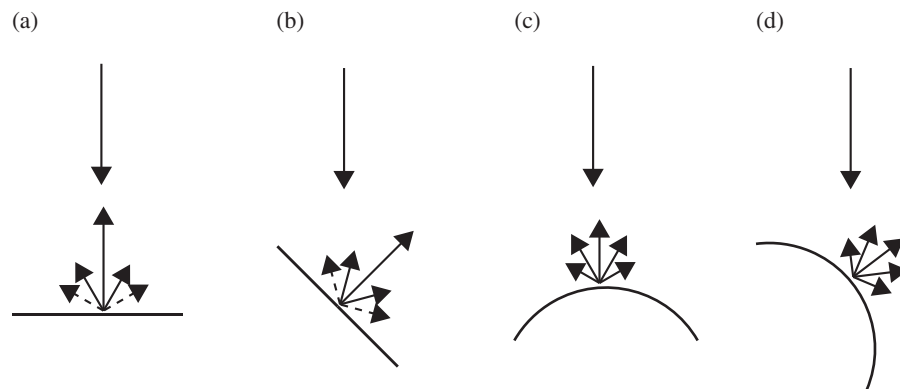


FIGURE 1.24 (a) An ideal surface, where most of the energy is reflected back to the transducer (high amplitude echo). (b) An ideal surface but at an angle of 45°, which will reflect most of the energy away from the surface (very low amplitude echo). (c) A curved surface that is a scatterer because it spreads out energy in all directions (low amplitude signal). (d) A curved surface that is perpendicular to the US beam; it is also a scatterer but more energy is reflected back to the beam.

size and direction of the signals, which in turn affects the type of scatters produced. It is important to note that the amplitude of the reflected signal, that is, the energy, is dependent on both the direction of the reflected signals and the reflection coefficient [44].

In ultrasound, the waves are attenuated when they are reflected and scattered in the tissue as well as when they are reflected and passed back to the probe. Typically, there is a 10% loss of total energy. The total energy decreases with penetration because there is an increase in energy lost the deeper the sound waves travel into the tissues because the sound waves are absorbed. Absorption in tissues is the most important cause of attenuation.

Absorption is extremely important in ultrasound for two reasons: depth penetration and safety concerns, the latter of which is the major limiting factor for its use as an imaging modality. The heat produced from absorption changes the temperature of the surrounding tissues, making it a limitation in ultrasound equipment due to safety issues for patients. The other is penetration issues because the attenuation of the US waves increases with depth. There are many factors that affect absorption such as the density of tissue and the frequency of the ultrasound beam. Good absorption generally results from high tissue density and sound frequency; hence penetration can be increased by increasing the transmitted energy. However, there are side effects such as tissue damage due to the extreme heat generated.

There are other types of ultrasound such as 3D ultrasound and Doppler ultrasound imaging based on the Doppler Effect. 3D imaging in general allows higher resolution imaging and thus provides more detailed information. This is commonly used to assess foetus development, as well as for biopsies. Doppler ultrasound is generally used for the study of the rate of blood flow through the heart and arteries [46].

There are many different ways to store ultrasound data, either in their full waveform as RF data that consist of both amplitude and frequency data or in pulse form where only data of the amplitude are collected and is less demanding on the storage systems. The signals can also be stored by taking the spectrum of frequencies from the reflected ultrasound pulse, which is then represented as a numerical value per image pixel. This method of storage is commonly used in Doppler imaging.

1.7.2 Advantages and Limitations

Ultrasound imaging is virtually noninvasive; it is used in a variety of clinical settings, especially in obstetrics and gynaecology, cardiology, and cancer detection. One of its most important uses is in studying and monitoring foetal development. No radiation is used in ultrasound imaging and the procedure can be performed much faster than X-rays and other radiographic techniques. Its major limitation is its poor penetration: US waves have difficulty penetrating the bone because they attenuate when passing deeper into the body. The body is also acoustically homogeneous because it contains around 70% water, thus it is difficult to discriminate the interface between the tissue and blood, but real-time evaluation of blood flow is possible. In general, ultrasound generates more heat as the frequency increases, so the ultrasonic frequency has to be carefully monitored. The signal intensities can be enhanced by the intravenous injection of contrast agents such as microbubbles at very low dosage, allowing the technique to remain minimally invasive.

Nevertheless, there are still safety concerns because the local temperature of tissue increases because heat is developed when the tissue or water absorbs the ultrasound energy. This local heat can also cause formation of cavitation.

Additionally, microbubbles have low circulation residence times and are easily taken up in certain locations—for example, the liver and the spleen—and can be destructed, inducing local microvasculature ruptures. Image enhancement can generally be improved by having high acoustic power output, but this again has to be compromised with the contrast agents, because high mechanical indices as well as low ultrasound frequencies tend to cause the microbubbles to burst. However, such properties can be beneficial for therapeutic purposes: Some studies have shown that the destructive nature of the microbubbles can be exploited for drug targeting and delivery. Despite concerns over the technique, US imaging is the most efficient technique with regard to cost, time, and safety compared to other imaging modalities such as MRI, PET, and SPECT, making it one of the most frequently used diagnostic techniques. Recent developments in ultrasound imaging have improved the resolution as well as the technique itself, allowing it to be incorporated into other methods such as photoacoustic imaging, a technique that uses the properties of both light and sound.

1.8 CONCLUSIONS

This chapter gives an overview of some of the most common imaging modalities and their basic principles. Their advantages and disadvantages are summarised in Figure 1.25, and a more detailed comparison is shown in Table 1.4. Each imaging modality has its own strengths and weaknesses for a particular area—for example, some techniques are more suited for cellular, molecular, or anatomic imaging—and in fact, many of these techniques are complementary. These detection systems differ in cost, availability, technical expertise needed, sensitivity, accuracy, and signal detection efficiency. Thus, the key issues depend on the type of research questions being addressed.

However, advancement in imaging technology has enabled the creation of multimodal imaging platforms, which has solved some of the dilemmas regarding the decision on what techniques should be used. At the same time, multimodal imaging helps to resolve time and cost issues. Multimodal imaging modalities are an attractive solution, especially in the area of diagnosis and in monitoring therapeutic responses; CT-MRI and CT-PET are already commonly used. The developments of new techniques are continuously being explored, so it is likely that multimodal imaging modalities will continue to be an area of interest, especially in the next decade. However, beneath this surface excitement around the advancement of new technology, a key influencing element in imaging is still in the area of developing molecular design and understanding their chemical properties. The demand for better imaging agents and probes parallels the development of new instrumentation. The need to overcome and comply with the endless hurdles concerning biological barriers and new mutagenic developments in diseases requires a constant need to review amplification strategies as well as to develop new molecular designs for better probes and contrast agents. There will be a continued search for creating specialised and specific probes propagated by endless, and as yet unknown, questions in areas such as oncology, physiology, and pathology.

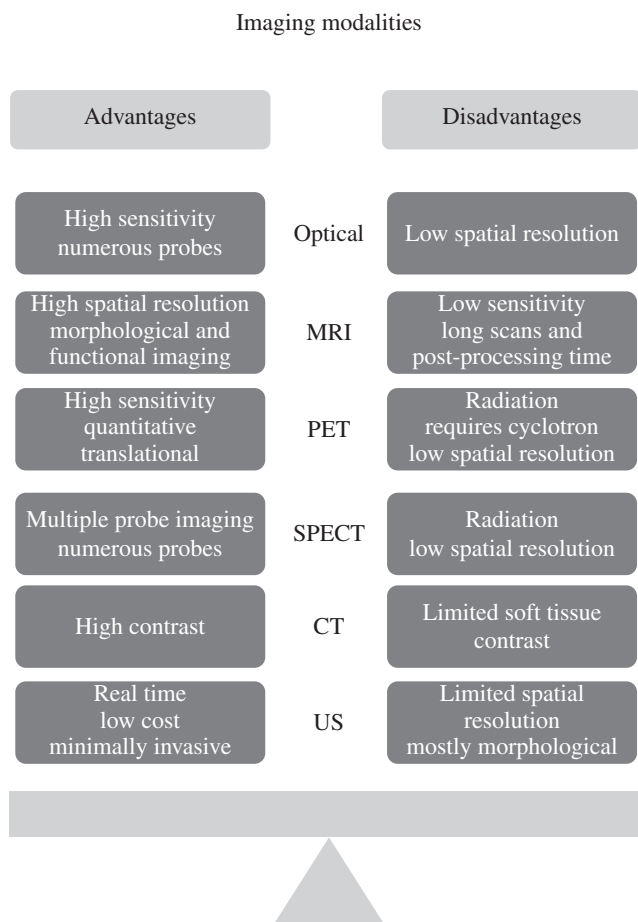
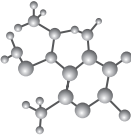







FIGURE 1.25 Pros and cons of different imaging modalities.

TABLE 1.4 Comparison of the Different Imaging Modalities

Imaging technique	Optical	MRI	PET	SPECT	X-ray CT	Ultrasound	Use of current imaging modalities
Type of electromagnetic radiation energy used in image generation	Visible to near infrared	Radiowaves	High energy γ rays	Lower energy γ rays	X-rays	High frequency sounds	Molecular
Spatial resolution	1.5–1000 nm	4–100 μ m ~1 mm-fMRI	1–2 mm	1–2 mm	12–50 μ m 50–200 μ m	50–500 μ m	
Depth	< 1 cm	No limit	No limit	No limit	No limit	mm to cm	Metabolism
Scan time	Seconds	Minutes to hours seconds to minutes-fMRI	Minutes	Minutes	Minutes	Seconds	 
Type of molecular probe and quantity of probes used	Activatable, direct or indirect micrograms to milligrams	Activatable, direct or indirect micrograms to milligrams	Radiolabeled, direct or indirect nanograms	Radiolabeled, direct or indirect nanograms	Limited activatable, direct micrograms to milligrams	Limited activatable, direct micrograms to milligrams	Physiology
Imaging agents- Contrast agents and molecular probes (Most of the imaging agents can be found from the Molecular Imaging and Contrast Agent Database (MICAD))	5-Carboxy-fluorescein, fluorescein, FITC, Alexa Fluor 488 and 647, 680, 750, Oregon Green 488 Cy5, Cy5.5 Cy7 Rhodamin X, Rhodamin Green, Luciferin, GFP IR-783, IR-786, IRDye78, IRDye800CW, NIR2, Quantum dot, Single walled carbon nanotubes, Ln based molecular dyes	Gadolinium based contrast agents- Magnevist, Dotarem, Prohance, Gadovist, OptiMark, Eovist, Vasovist/Ablavar, Tm ³⁺ , ²³² F ⁻ , Manganese ferrite, Iron oxides	Technetium-99m: used mostly for bone and heart scans ²⁸ F-fluoromisonidazole/ ⁶⁴ Cu-ATSM-identify hypoxia in tissues, gallium-attaches to area of inflammation ²⁸ F-fluoride-imaging of new bone formation ²⁸ F-fluorodeoxyglucose (FDG) images the metabolic activity of tissues. Can identify cancerous cells.	^{99m} Tc 186Re, 188Re 111In, 123I, 125I, 131I, 170Tm, 177Lu,	Iodine contrast agents-highlights blood vessels as well as tissues of various organs Barium-images of the abdomen and pelvis Gastrografin	Microbubbles/nanobubbles Optison microbubbles-perfluoropropane gas encapsulated by a serum albumin shell Dyes and Glod	 
Key use	Visualisation of cell structures	Anatomical imaging and functional imaging of brain activity-fMRI	Metabolic imaging	Metabolic imaging	Lung and bone tumour imaging	Vascular imaging	Anatomy 

REFERENCES

- [1] H. R. Herschman, *Science* **302**, 605–608 (2003).
- [2] G. L. ten Kate, E. J. G. Sijbrands, R. Valkema, F. J. ten Cate, S. B. Feinstein, A. F. W. van der Steen, M. J. A. P. Daemen and A. F. L. Schinkel, *J. Nuclear Cardiology* **17**, 897–912 (2011).
- [3] F. Dalagija, A. Mornjaković and I. Sefić, *Acta Medica Academica* **35**, 35–39 (2006).
- [4] M. D. Seemann, *Eur. J. Med. Res.* **28**, 241–246 (2004).
- [5] T. Ido, C. N. Wan, V. Casella, J. S. Fowler, A. P. Wolf, M. Reivich and D.E. Kuhl, *J. Label. Compd. Radiopharm.* **14**, 175–182 (1978).
- [6] T. G. Tukington, *J. Nucl. Med. Technol.* **29**, 4–11 (2001).
- [7] M. M. Ter-Pogossian, M. E. Phelps, E. J. Hoffman and N. A. Mullani, *Radiology* **114**, 89–98 (1975).
- [8] N. Blow, *Nat. Meth.* **6**, 465–469 (2009).
- [9] O. Belohlavek, E. Bombardieri, R. Hicks and Y. Sasaki, *A Guide to Clinical PET in Oncology: Improving Clinical Management of Cancer Patients*, 2008, Chapter 1, 1–8.
- [10] S. M. Ametamey, M. Honer and P. A. Schubiger, *Chem. Rev.* **108**, 1501–1516 (2008).
- [11] A. K. Buck, S. Nekolla, S. Ziegler, A. Beer, B. J. Krause, K. Herrmann, K. Scheidhauer, H. J. Wester, E. J. Rummeny, M. Schwaiger and A. Drzezga, *J. Nucl. Med.* **49**, 1305–1319 (2008).
- [12] K. Schwochau, *Angew. Chem. Int. Ed. Engl.* **33**, 2258–2267 (1994).
- [13] G. F. Knoll, *Proceedings of the IEEE* **71**, 320–329 (1983).
- [14] R. J. Jaszczak, *Physics in Medicine and Biology* **51**, R99–R115 (2006).
- [15] M. M. Khalil, J. L. Tremoleda, T. B. Bayomy and W. Gsell, *Int. J. Mol. Imag.* 1–15 (2011).
- [16] W. C. Lively, S. Goetze, K. P. Friedman, J. P. Leal, Z. Zhang, E. Garret-Mayer, A. P. Dackiw, R. P. Tufano, M. A. Zeiger and H. A. Ziessman, *J. Nucl. Med.* **48**, 1084–1089 (2007).
- [17] N. J. Dougall, S. Bruggink and K. P. Ebmeier, *Am. J. Geriatr. Psychiatry* **12**, 554–570 (2004).
- [18] A. G. Filler, *Int. J. Neur.* **1**, (2010).
- [19] E. C. Lasser, C. C. Berry, L. B. Talner, L. C. Santini, E. K. Lang, F. H. Gerber and H. O. Stolberg, *N. Engl. J. Med.* **317**, 845–849 (1987).
- [20] D. J. Brenner and E. J. Hall, *N. Engl. J. Med.* **357**, 2277–2284 (2007).
- [21] G. T. Herman, *Fundamentals of Computerized Tomography: Image Reconstruction from Projection*. 2nd ed. Springer, 2009.
- [22] D. W. Townsend, *Annals Acad. Med.* **33**, 133–145 (2004).
- [23] <http://reference.medscape.com/features/slideshow/lung-cancer-staging>
- [24] R. V. Damadian, *Science* **171**, 1151–1153 (1971).
- [25] K. J. Murphy, J. A. Brunberg and R. H. Cohan, *AJR Am J Roentgenol.* **167**, 847–849 (1996).
- [26] W. R. Hendee and C. J. Morgan, *West. J. Med.* **141**, 491–500 (1984).
- [27] D. Le Bihan, E. Breton, D. Lallemand, P. Grenier, E. Cabanis and M. Laval-Jeantet, *Radiology* **161**, 401–407 (1986).
- [28] S. Aime, M. Botta, M. Fasano and E. Terreno, *Chem. Soc. Rev.* **27** 19–29 (1998).
- [29] W. B. Amos, J. G. White and M. Fordham, *Appl. Opt.* **26**, 3239–3243 (1987).
- [30] J. R. Lakowicz, *Principles of Fluorescence Spectroscopy*. 3rd ed. Springer, 2006.
- [31] A. T. R. Williams, S. A. Winfield and J. N. Miller, *Analyst* **108**, 1067–1071 (1983).
- [32] D. R. Sandison, D. W. Piston, R. M. Williams and W. W. Webb, *Appl. Opt.* **34**, 3576–3588 (1995).
- [33] W. B. Amos and J. G. White, *Biol. Cell* **95**, 335–342 (2003).
- [34] J. B. Pawley, *Handbook of Biological Microscopy*. Springer, 2006.
- [35] C. Preza, D. L. Snyder and J.-A. Conchello, *J. Opt. Soc. Am. A* **16**, 2185–2199 (1999).
- [36] J. B. de Monvel, S. Le Calvez and M. Ulfendahl, *Biophysical* **80**, 2455–2470 (2001).
- [37] J. W. Lichtman and J.-A. Conchello, *Nat. Meth.* **2**, 910–919 (2005).
- [38] C. Kaminski and J. R. Soc. *Interface* **6**, S1–S2 (2009).
- [39] F. Helmchen, *Exp. Phys.* 738–745 (2011).
- [40] P. N. T. Wells, *Phys. Med. Biol.* **51**, R83–R98, (2006).
- [41] P. N. T. Wells, *Rep. Prog. Phys.* **62**, 671–722 (1999).
- [42] M. S. Hughes, G. M. Lanza, J. N. Marsh and S. A. Wickline, *MedicaMundi* **47**, 66–73 (2003).
- [43] D. Cosgrove, *Eur. J. Radiol.* **60**, 324–330 (2006).
- [44] K. G. Baker, V. J. Robertson and F. A. Duck, *Phys. Ther.* **81**, 1351–1358 (2001).
- [45] R. S. C. Cobbold, *Foundations of Biomedical Ultrasound*. Oxford University Press, 2007.